Biochimica et Biophysica Acta 932 (1988) 232–239
Elsevier

BBA 42706

Changes in the apparent affinity of CF_0-CF_1 for its substrates during photophosphorylation

W. Paul Quick and John D. Mills

Department of Biological Sciences, University of Keele, Keele, Staffs. (U.K.)

(Received 18 August 1987)

Key words: Photosynthesis; Chloroplast; ATP synthesis; Chemiosmotic hypothesis; Uncoupler; Energy transfer inhibitor

The apparent K_m value for inorganic phosphate (P_i) of the chloroplastic ATPase has been measured under different conditions of light intensity, uncoupler concentration and energy-transfer inhibitor concentration. Systematic changes in the values were observed which were similar to but not identical with reported changes in the K_m for ADP under similar conditions (Quick, W.P. and Mills, J.D. (1987) Biochim. Biophys. Acta 893, 197–207). Both sets of experimental data could be simulated using a mathematical model based on: (a) Michaelis–Menten kinetics of the ATPase with respect to ADP and P_i; and (b) delocalised chemiosmotic energy coupling. We conclude that the changes observed in the K_m are a result of systematic changes in the protonmotive force during the K_m analysis.

Introduction

The detailed mechanism by which the chloroplast ATPase (CF_0-CF_1) catalyses reversible ATP synthesis is still not known. Three adenine nucleotide binding sites can be detected on the catalytic portion of the ATPase (CF_1) [1] and it has been proposed that these act cooperatively during catalysis [2]. Despite this, a simple hyperbolic relationship is observed between the rate of light-driven ATP synthesis and the concentration of substrate ADP, allowing a K_m and V to be calculated from double reciprocal plots [3–7]. That these plots are linear is all the more remarkable in view of the fact that photophosphorylation depends not only on the chloroplast ATPase but also on efficient energy coupling to the reactions of light-driven electron transport.

In view of this complexity, it is not surprising that the observed values of K_m and V for ADP during photophosphorylation depend on the conditions of measurement. It has been widely observed that both lowering the light intensity and adding of uncoupler decrease V but have opposite effects on K_m [3–6], but see Ref. 7. Since the direction of the change in K_m correlated with changes in the rate of electron transport, it was suggested [3,5] that there existed direct links between electron transport and ATPases, and that energy coupling may not occur via a simple, delocalised electrochemical potential difference of protons across the membrane as envisaged in Mitchell's chemiosmotic hypothesis [8]. In a recent paper, we confirmed and extended these K_m observations to include estimates of the steady-state ΔpH during the experiments [6]. It was shown that ΔpH was a variable that decreased in magnitude during the K_m analysis as ADP concentra-

Abbreviations: P_i, inorganic phosphate; Tricine, *N*-[2-hydroxy-1,1-bis(hydroxymethyl)ethyl]glycine.

Correspondence: W.P. Quick, Department of Biological Sciences, University of Keele, Keele, Staffs., ST5 5BG, U.K.

tions were increased. It was therefore suggested that this systematic variable caused the observed K_m to be underestimated and that changes in ΔpH upon lowering light intensity or partial uncoupling were hence able to account for the observed changes in K_m. In support of this idea, a mathematical model was presented [6], based on simple Michaelis–Menten kinetics of the ATPase with respect to ADP and delocalised energy coupling.

If this explanation for the observed changes in K_m for ADP is correct, then it is predicted that the observed K_m for inorganic phosphate (P_i) should exhibit similar behaviour to that observed for ADP. A wide range of values [9–14] have been reported for $K_m(P_i)$ in the literature but the source of the variation has not been systematically investigated. In this paper we have characterised the response of the apparent K_m for P_i to the experimental conditions and have extended a mathematical model for photophosphorylation, described previously [6], to incorporate both ADP and P_i as substrates. It is shown that the apparent K_m for P_i is altered by changes in the experimental conditions in a manner similar to those reported for the apparent K_m for ADP. Both sets of data can be simulated using a mathematical model that assumes simple two-substrate Michaelis–Menten kinetics with respect to ADP and P_i. We conclude that the observed complex behaviour of the apparent K_m is primarily due to the response of the protonmotive force to changes in the balance of proton fluxes across the thylakoid membrane, and is thus a predicted and logical consequence of a delocalised chemiosmotic mechanism. The physiological significance of these effects is also considered.

Materials and Methods

Experimental

Intact chloroplasts were isolated from *Pisum sativum* (variety Feltham First) and then lysed and washed prior to a final resuspension according to a method described previously [15]. Chloroplasts were isolated from dark-adapted plants and experimentation was completed within 3 h of preparation. To compensate for any loss of ATPase activity over the period of the experiment results were calculated as an average of duplicate experiments carried out in reverse order.

The rate of ATP synthesis and the magnitude of the transthylakoid pH gradient were measured simultaneously from thylakoids suspended in a medium containing 20 mM KCl, 5 mM $MgCl_2$, 0.1 mM methyl viologen, 15 mM glucose, 10 units/ml hexokinase, 2.5 μg/ml diadenosine pentaphosphate, 20 μM 9-aminoacridine, 1000 units/ml catalase, 0.4 μCi $^{32}P_i$ (Amersham International) and 30 mM Tricine-KOH (pH 8.1) in an oxygen electrode maintained at 20 °C. For determination of the apparent K_m for ADP, 1 mM P_i was included in the medium and the concentrations of ADP used were 3, 5, 8, 12, 18 and 25 μM, respectively. For determination of the apparent K_m for P_i, 1 mM ADP was included in the medium and the final concentrations of P_i used were 64, 74, 94, 124, 194 and 294 μM, respectively. This included a background P_i contamination of the medium which was measured to be 44 ± 4 μM.

Illumination was provided by a Halogen lamp filtered through a Corning RG665 red-pass filter. ΔpH was estimated using 9-aminoacridine fluorescence and was measured as described previously [15]. Photophosphorylation was initiated by illumination and was terminated by the addition of 200 μl 20% trichloroacetic acid to 1 ml of assay medium containing 15 μg of chlorophyll (unless otherwise indicated). An illumination period of 2 min was used when determining the K_m for ADP but this was reduced to 30 s and the chlorophyll reduced to 7.5 μg when determining the K_m of P_i in order to minimise any changes in the P_i concentration that could occur during the assay period. Less than 6% of the available P_i was calculated to be consumed during the experiment. The ADP concentration was maintained during the assay by enzymic recycling; the concentration of ADP under steady-state phosphorylating conditions, as determined by the luciferin-luciferase technique, was always within 10% of the initial ADP concentration. The rate of ATP synthesis was determined by $^{32}P_i$ incorporation into glucose 6-phosphate as described previously [15].

The rate of ATP synthesis was varied by: (a) reducing the light intensity with neutral density filters; (b) the addition of the uncoupler nigericin; or (c) the addition of the energy-transfer inhibitor

tentoxin (Sigma Chemical Company) (concentrations were as indicated). Due to the slow inhibition kinetics of tentoxin, especially at low concentrations, thylakoids were preincubated in the assay medium for 20 min at 20 °C with the appropriate tentoxin concentration prior to illumination.

The data are presented as the K_m and V values obtained from Lineweaver–Burk plots; a line of best fit was calculated on a microcomputer using a linear regression technique and correlation coefficients were always greater than 0.95.

Theoretical

Theoretical data were calculated from a mathematical model designed to simulate photophosphorylation using simple pathways of proton flux. The model presented assumes Michaelis–Menten kinetics for CF_0-CF_1 with respect to both ADP and P_i, and is an extension of a model previously presented [6], and based on earlier models of photophosphorylation at saturating substrate concentrations [16,17]. An outline of the model is shown in Scheme I and is explained further in the discussion.

This scheme is expressed mathematically in Eqn. 1 below.

$$(E_a \cdot H_3 \cdot [\mathrm{ADP}] \cdot [\mathrm{P_i}])K_5 = v = \frac{V_p}{1 + C + (1+B)\frac{K_{m\,P_i}}{[\mathrm{P_i}]} + (1+A)\left\{\frac{K_{m\,P_i}}{[\mathrm{ADP}]} \cdot \frac{KSA}{[\mathrm{P_i}]} + \frac{K_{m\,ADP}}{[\mathrm{ADP}]}\right\}} \quad (1)$$

where

$K_{m\,ADP}$ = $K_5/K_1 = 12$ μM

$K_{m\,P_i}$ = $(K_4 + K_5)/K_3 = 200$ μM

KSA = $K_2/K_1 = 12$ μM

K_6/K_7 = 0.05

K_8/K_9 = 0.1

K_{10}/K_{11} = 0.025

$A = \frac{K_6}{K_7}\left\{1 + \left(\frac{K_{p1}}{H^+_{in}} \cdot \frac{H^+_{out}}{K_{n1}}\right)\right\}^3$

$B = \frac{K_8}{K_9}\left\{1 + \left(\frac{K_{p2}}{H^+_{in}} \cdot \frac{H^+_{out}}{K_{n2}}\right)\right\}^3$

$C = \frac{K_{10}}{K_{11}}\left\{1 + \left(\frac{K_{p3}}{H^+_{in}} \cdot \frac{H^+_{out}}{K_{n3}}\right)\right\}^3$

$[P_i]$ = concentration of P_i (μM), value as indicated in text

[ADP] = concentration of ADP (μM), value as indicated in text

H^+_{out} = external proton concentration, set at $1 \cdot 10^{-8}$ M

H^+_{in} = internal proton concentration calculated such that Eqn. 4 is satisfied

K_{p1}, K_{p2}, K_{p3} = $1 \cdot 10^{-5}$ M, internal dissociation constant of CF_0-CF_1, see Ref. 13 for discussion

K_{n1}, K_{n2}, K_{n3} = $1 \cdot 10^{-8}$ M, external dissociation constant of CF_0-CF_1, see Ref. 13 for discussion.

Three proton flux equations were constructed to simulate steady-state photophosphorylation (Eqns. 2–4).

$$J_{H^+_{in}} = V_e \frac{K_a}{K_a + H^+_{in}} \quad (2)$$

$$J_{H^+_{out(P)}} = pv \quad (3)$$

$$J_{H^+_{out(nP)}} = H^+_{in} C \quad (4)$$

$$J_{H^+_{in}} = J_{H^+_{out(P)}} + J_{H^+_{out(nP)}} \quad (5)$$

where

$J_{H^+_{in}}$ = the inward flux of protons due to electron transport

$J_{H^+_{out(nP)}}$ = the outward flux of protons due to membrane leakage

$J_{H^+_{out(P)}}$ = the outward flux of protons due to photophosphorylation

C = passive permeability constant for diffusion of protons across thylakoid membrane, value set as indicated in text

V_p = maximum rate of ATP synthesis, value set as indicated in text

p = H^+/ATP ratio, set at 3

V_e = maximum rate of uncoupled electron-transport-driven proton translocation, value as indicated in text

K_a = acid dissociation constant of an internal group controlling electron transport, set at $1 \cdot 10^{-5}$ M.

All proton fluxes are expressed as μmol per mg chlorophyll per h.

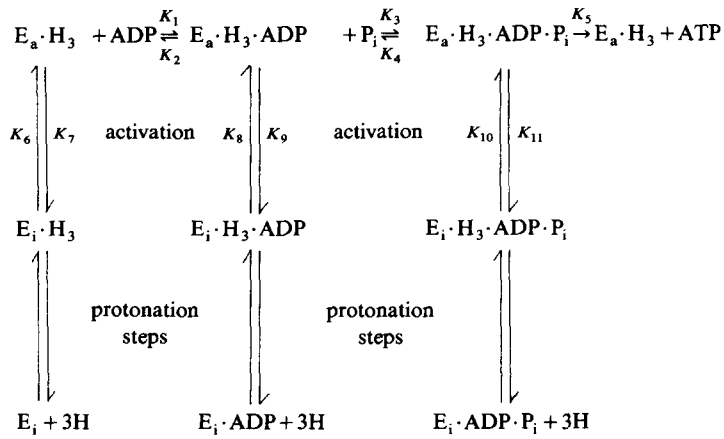

Scheme I. Kinetic scheme for CF_0-CF_1-catalysed ATP synthesis.

Eqn. 2 describes the influx of protons due to electron transport and incorporates a term to describe the ΔpH-dependent feedback inhibition of electron transport [15]. Eqn. 3 describes the proton efflux due to phosphorylation (P) and assumes Michaelis–Menten kinetics with respect to ADP and P_i and incorporates a $\Delta\mu_{H^+}$-dependent activation of the ATPase. Eqn. 4 describes the non-phosphorylating efflux of protons (nP) due to membrane leakage which is assumed to be directly related to the internal proton concentration [18].

The external proton concentration (H^+_{out}) was maintained as a constant and the internal proton concentration was varied until the proton flux equations (Eqns. 2–4) satisfied Eqn. 5; this was solved using a computer iteration technique. Constants used in the model were manipulated in order to simulate experimental conditions; the extent of uncoupling was simulated by varying the value of C, the rate of electron transport was simulated by altering the value of V_e and the extent of energy-transfer inhibition was simulated by altering the value of V_p. All other constants in the model were kept the same for all the theoretical data presented.

A Lineweaver–Burk plot of model data showed a slight non-linearity when the values of [ADP], P_i], V_e and V_p were large and C was small. In order to compensate for this small but potential artifact the model K_m and V values were calculated from substrate concentrations used experimentally and a linear regression technique was used to calculate a line of best fit; correlation coefficients were always greater than 0.99. The intercepts of this line with the x- and y-axis were then used to determine the apparent K_m and V values.

Results

In agreement with others, we found that a simple hyperbolic relationship existed between the observed rate of ATP synthesis and the concentration of substrate P_i in the medium, allowing a K_m and V to be estimated from double reciprocal plots. As shown in Fig. 1, these plots remained linear under different experimental conditions. It can be seen that a reduction in light intensity from 240 to 53 W/m^2 caused both K_m and V to be lowered, whereas addition of a subsaturating concentration of nigericin (60 nM) also lowered V but increased the apparent K_m. Both treatments inhibited V by approx. 50%.

In a previous paper, it was argued that similar changes in the observed K_m for ADP could be explained by systematic changes in ΔpH that occurred during the K_m analysis [6]. Fig. 2 shows how the estimated ΔpH value varied according to the phosphate concentration in the assay medium under similar conditions to those used in the experiments depicted in Fig. 1. At saturating light intensity the ΔpH progressively declined as the P_i concentration was increased. At low light intensity a lower average ΔpH value was observed but the

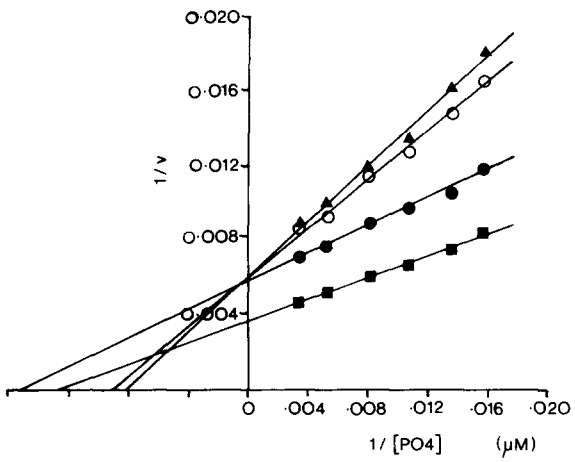

Fig. 1. Lineweaver–Burk plots of the rate of light-driven ATP synthesis (v) against substrate P_i. Squares represent high light intensity (240 $W \cdot m^{-2}$). Other conditions were as follows: closed circles, 53 $W \cdot m^2$; open circles, plus 60 nM nigericin; triangles, plus 48 nM tentoxin.

extent to which ΔpH changed upon increasing P_i concentration remained the same as for saturating light intensity. The addition of nigericin also lowered the average ΔpH value to a similar level as the reduced light intensity. However, the change in ΔpH due to increased P_i concentration was markedly reduced. As discussed later, these changes in ΔpH are similar to those that occur when ADP is the varied substrate [6] and can account for the apparent K_m changes.

Fig. 3A shows the experimentally observed relationship between the apparent K_m and V for substrate P_i when the rate was varied over an extended range of light intensities and uncoupler concentrations. Fig. 3A shows that upon reducing the light intensity, both V and K_m values are

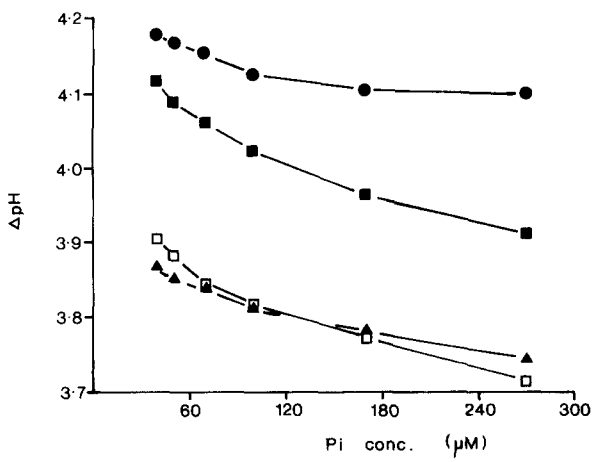

Fig. 2. The magnitude of the transthylakoid pH gradient (ΔpH) estimated from the quenching of 9-aminoacridine fluorescence as a function of the P_i concentration. The light intensity was 240 $W \cdot m^{-2}$ (solid symbols) or 53 $W \cdot m^{-2}$ (open symbols). 50 nM nigericin (triangles) or 48 nM tentoxin (circles) were included in the assay medium. Chloroplasts were preincubated for 20 min in the dark at a concentration of 5 μg per ml in assay medium prior to determination of the ΔpH.

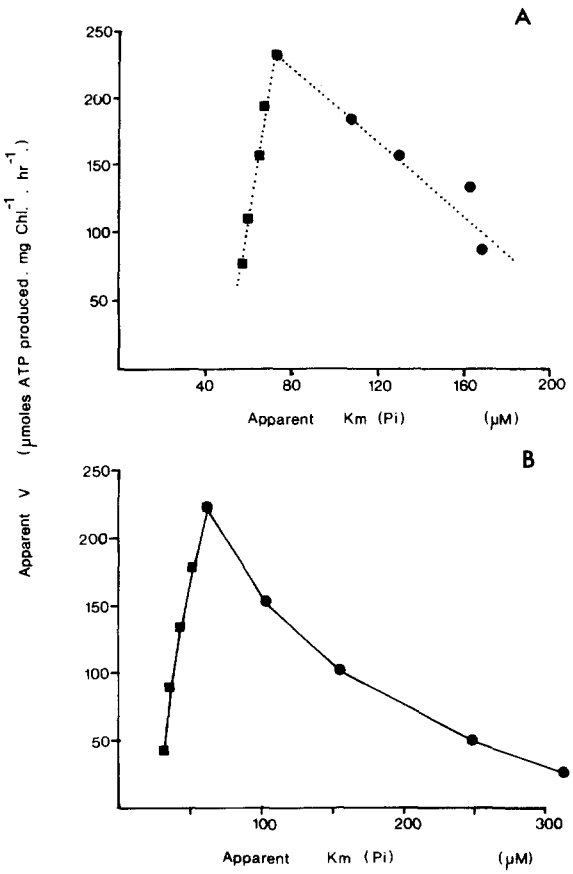

Fig. 3. Relationship between V and K_m of CF_0-CF_1 for P_i at different light intensities and uncoupler concentrations (A) determined experimentally or (B) calculated from a mathematical model. In (A) squares represent decreasing light intensity (240, 120, 53, 29, 19 $W \cdot m^{-2}$) and circles represent increasing nigericin concentration (0, 30, 60, 80, 120 nM) from the top to the bottom of the graph. In (B) squares represent decreasing values of V_e (1000, 800, 600, 400, 200) and circles represent increasing values of C ($2 \cdot 10^7$, $1 \cdot 10^8$, $2 \cdot 10^8$, $4 \cdot 10^8$, $6 \cdot 10^8$) from the top to the bottom of the graph. V_p was set at 833 and ADP was maintained at 1 mM.

lowered and there appears to be a linear relationship between the two values with a clearly non-zero intercept on the K_m-axis. However, when the apparent value of V was reduced by increased uncoupler concentration there was a marked increase in the apparent K_m value. Fig. 4A shows that these data are similar to, but not identical with, changes in the observed K_m and V for ADP measured under similar conditions. In the latter case, the relationship between K_m and V is rather more non-linear, and the pattern of the curves appears to be rotated anticlockwise relative to the P_i data.

The data of Fig. 4A have previously been reported and were shown to be simulated by a mathematical model that assumed Michaelis-Menten kinetics with respect to ADP and a delocalised chemiosmotic energy coupling mechanism [6]. We now report that an extended version of this model can simultaneously predict both the ADP and P_i sets of experimental data. The model

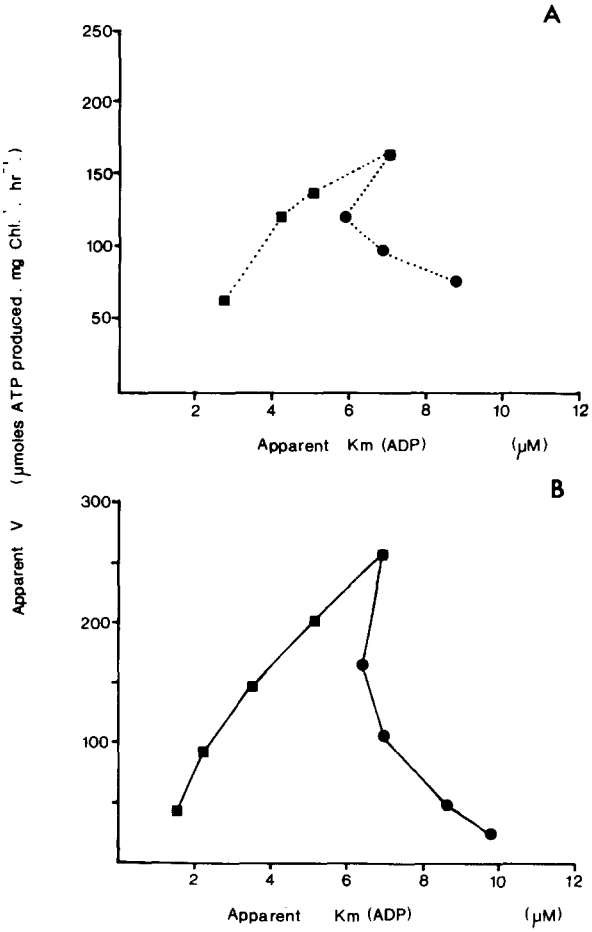

Fig. 4. Relationship between V and K_m of CF_0-CF_1 for ADP at different light intensities and uncoupler concentrations determined experimentally (A) or calculated from a mathematical model (B). In (A) squares represent decreasing light intensity (240, 110, 53, 29 $W \cdot m^2$) and circles represent increasing nigericin concentration (0, 30, 60, 90 nM) from the top of the bottom of the graph. In (B) squares represent decreasing values of V_e (1000, 800, 600, 400, 200) and circles represent increasing values of C ($2 \cdot 10^7$, $1 \cdot 10^8$, $2 \cdot 10^8$, $4 \cdot 10^8$, $6 \cdot 10^8$) from the top to the bottom of the graph, V_p was set at 833 and P_i was maintained at 10 mM.

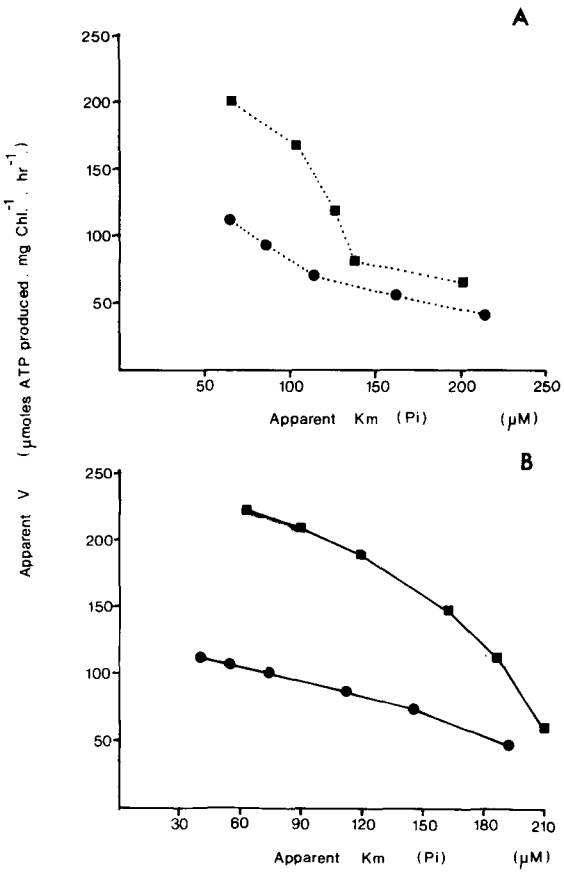

Fig. 5. Relationship between V and K_m of CF_0-CF_1 for P_i at two light intensities and different energy transfer inhibitor concentrations determined experimentally (A) or calculated from a mathematical model (b). In (a) the light intensities were 240 $W \cdot m^{-1}$ (squares) or 53 $W \cdot m^{-2}$ (circles) and the concentration of tentoxin was 0, 48, 96, 144, 192 nM, respectively from the top of the bottom of the graph. In (b) $V_e = 1000$ (squares) or $V_e = 500$ (circles), $C = 2 \cdot 10^7$, ADP = 1 mM, and $V_p = 833$, 667, 500, 250, 167 and 83, respectively, from the top to the bottom of the graph.

assumes a two-substrate reaction mechanism for CF_0CF_1, involving a compulsorily ordered binding of ADP prior to P_i. Under a single set of assumptions for numerical constants, the model can simulate experimental data for both P_i (Fig. 3b) and ADP (Fig. 4b), simply by decreasing V_e to simulate a decrease in light intensity or by increasing the value of C to simulate increased uncoupling.

In a further effort to characterise the response to changes in experimental conditions, we studied the effect of an energy-transfer inhibitor (tentoxin) on the apparent V and K_m values of CF_0-CF_1 for P_i (Fig. 5). As shown in Fig. 1 and in more detail in Fig. 5A, the apparent K_m for P_i is increased markedly by tentoxin inhibition at both high and low light intensity. Again, this response was observed in the theoretical data (Fig. 5B) where energy-transfer inhibition was simulated by lowering the value of V_p and two values of V_e were used to simulate different light intensities. These data are similar to previous reports from this laboratory on the effects of energy-transfer inhibition on the apparent K_m for ADP.

Discussion

The experimental data presented here demonstrate that the apparent Michaelis–Menten constant (K_m) of CF_0-CF_1 for its substrate P_i varies according to the experimental conditions in a manner similar to the apparent K_m for ADP reported earlier [6]. In general when the value of V is reduced by lowering the light intensity the apparent K_m for P_i is decreased, but when V is reduced by the addition of uncouplers then the apparent K_m is increased. Both treatments lower the overall ΔpH but have opposite effects on the rate of electron transport. In contrast, energy transfer inhibition, which results in an enhanced ΔpH and a lower rate of electron transport (data not shown), also causes the apparent K_m for P_i to increase as the value of V is reduced. Thus, there is no correlation between the direction of change of the K_m with either the direction of change of ΔpH or the rate of electron trnasport and thus there is no circumstantial evidence to justify the proposal of direct links between ATPases and electron-transport chains.

We previously explained the changes in the apparent K_m for ADP in terms of changes that occur in the magnitude of the ΔpH during the K_m analysis [6], and offer the same explanation for observed changes in $K_m(P_i)$. According to this idea, the ΔpH is uncontrolled during the experiment and will tend to decrease as the concentration of substrate increases. The systematic changes in ΔpH will lead to an underestimation of the true K_m. Upon lowering light intensity, this systematic change in ΔpH is exacerbated causing the observed K_m to decrease further. However, addition of uncoupler or energy-transfer inhibitor causes phosphorylating proton efflux to diminish in magnitude relative to phosphorylating efflux. ΔpH is now less responsive to increases in substrate and the K_m appears to increase from its (artifactually) low value.

Supporting these ideas, we have shown that a simple mathematical model of photophosphorylation can produce results in close agreement with those obtained experimentally. The model assumes two substrate Michaelis-Menten kinetics with respect to ADP and P_i and contains terms which allow for $\Delta\mu_{H^+}$-dependent activation of the various enzyme intermediates. The model is the simplest mathematical description of delocalised photophosphorylation that we could devise which could predict the experimental data. The mechanistic description of ATP synthesis assumed in the model is an obvious over-simplification, since it does not account for the involvement of three nucleotide binding sites. The most important aspect of the model is that it encompasses the whole system of photophosphorylation and hence the relationships between ΔpH and the various pathways of proton flux. That the model can predict the data emphasises that the K_m changes are primarily a system response rather than an indicator of ATPase mechanism.

However, it may be significant that the experimental data shows the apparent K_m for ADP to be more sensitive to a reduction in light intensity than the apparent K_m for P_i; the reverse is true in the presence of uncouplers. In order to model this result we had to assume that values for the stability of the $\Delta\mu_{H^+}$-activated forms of the various enzyme-substrate intermediates were different, notably that the Enz-ADP-P_i complex were more

stable than the Enz-ADP complex. The validity of this assumption and its possible consequence for the mechanism of activation of CF_0-CF_1 are currently under investigation.

Finally, the in vivo concentration of adenine nucleotides and P_i within the chloroplast stroma are generally in the millimolar range. Even though it has been reported that stromal proteins can act as energy-transfer inhibitors [12], it is unlikely from the values of K_m reported here that changes in the affinity of CF_0-CF_1 for its substrates under different conditions will contribute to the regulation of photosynthesis in vivo.

Acknowledgements

Nigericin was a kind gift from the Eli Lilly Corporation. We thank G.B. Burgess for his help in the preparation of the manuscript and we are grateful to the SERC for financial support of this work.

References

1 McCarty, R.E. and Hammes, G.G. (1987) Trends Biochem. Sci. 12, 234–237.
2 Kuhlbrenner, W.E. and Boyer, P.D. (1983) J. Biol. Chem. 258, 10881–10886.
3 Vinkler, C. (1981) Biochem. Biophys. Res. Commun. 99, 1095–1100.
4 Bickel-Sandkötter, S. and Strotmann, H. (1981) FEBS Lett. 125, 188–192.
5 Loehr, A., Willms, I. and Huchermeyer, B. (1981) Arch. Biochem. Biophys. 236, 832–840.
6 Quick, W.P. and Mills, J.D. (1987) Biochim. Biophys. Acta 893, 197–207.
7 Davenport, J.W. and McCarty, R.E. (1986) Biochim. Biophys. Acta 851, 136–145.
8 Mitchell, P. (1979) Eur. J. Biochem. 95, 1–20.
9 Selman, B.R. and Selman-Reimer, S. (1981) J. Biol. Chem. 256, 1722–1726.
10 Aflalo, C. and Shavit, N. (1983) FEBS Lett. 154, 175–178.
11 Junge, W., Schoenknecht, G. and Lill, H. (1987) in Progress in Photosynthesis Research (Biggins, J., ed.), Vol. III, pp. 133–140, Martinus Nijhoff, Dordrecht.
12 Furbank, R.T., Foyer, C.H. and Walker, D.A. (1986) Biochim. Biophys. Acta 852, 46–54.
13 Kayalar, C., Rosing, J. and Boyer, P.D. (1976) Biochem. Biophys. Res. Commun. 72, 1153–1159.
14 Hatefi, Y., Yagi, T., Phelps, D.C., Wong, S., Vik, S.B. and Galante, Y.M. (1982) Proc. Natl. Acad. Sci. USA 99, 1756–1760.
15 Mills, J.D. (1986) in Photosynthesis Energy Transduction (Hipkins, M.F. and Baker, N.R., eds.), Ch. 6, pp. 143–186, IRL press, Oxford
16 Mills, J.D. and Mitchell, P. (1984) in Advances in Photosynthesis Research (Sybesma, C., ed.), Vol. II, pp. 523–526, Martinus Nijhoff/Dr. W. Junk Publishers, Dordrecht.
17 Mills, J.D. and Mitchell, P. (1984) Biochim. Biophys. Acta 764, 93–104.
18 Portis, A.R. and McCarty, R.E. (1976) J. Biol. Chem. 251, 1610–1617.